

# ALOS Interferometry of the the M<sub>w</sub> 7.9 Wenchuan Earthquake: ScanSAR-to-ScanSAR

Xiaopeng Tong, David Sandwell, Scripps Institution of Oceanography, La Jolla, CA 92093-0225  
 Rob Mellors, San Diego State Univ. San Diego, CA, 92182-1020

## (1) Introduction

On May 12<sup>th</sup> 2008, a major (M<sub>w</sub>7.9) earthquake occurred along the eastern boundary of the Tibetan plateau in the Sichuan province of China. Shaking from the 270 km long rupture of faults of the Longmen Shan destroyed thousands of structures killing nearly 70,000 people and leaving more than 4.8 million homeless. Understanding the time variations in the crustal stresses associated with the co- and post-seismic deformation from this earthquake will be important for seismic hazard analysis in the region. The rupture occurred in an area of extreme topography, moderate vegetation, and high rainfall which necessitate the use of longer wavelength L-band radar to retain phase coherence.

Significant displacements from this earthquake cover an area 400 km by 400 km. The spatial and temporal coverage from ALOS PALSAR is excellent but recovery of the full deformation field requires new multipass strip mode combination methods as well as pixel offset measurements and ScanSAR interferometry. GPS measurements will be needed to monitor the regional variations in postseismic deformation. Models of postseismic deformation, driven by the co-seismic stress perturbation, will provide important information on hazards from future earthquakes and aftershocks.

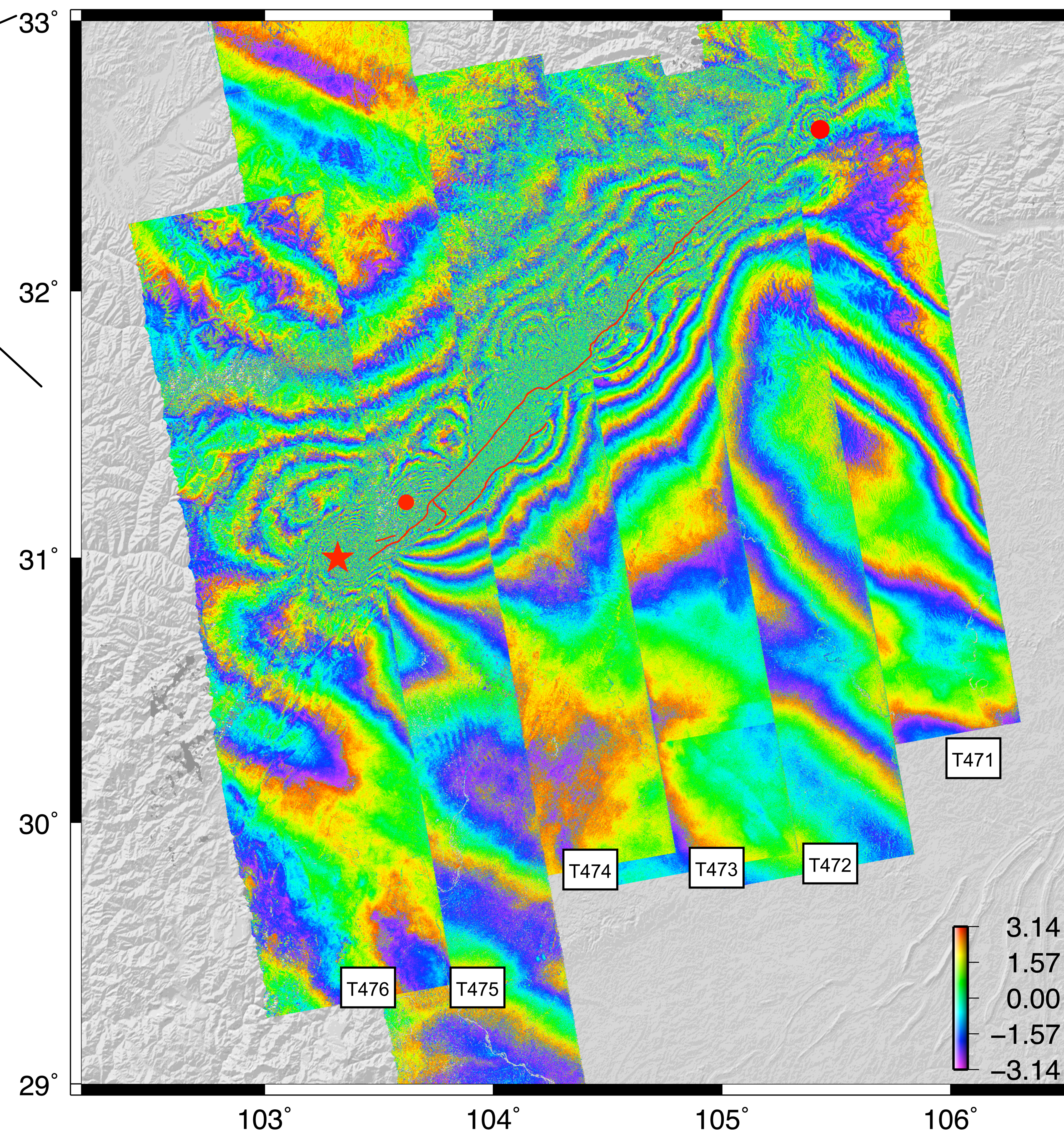
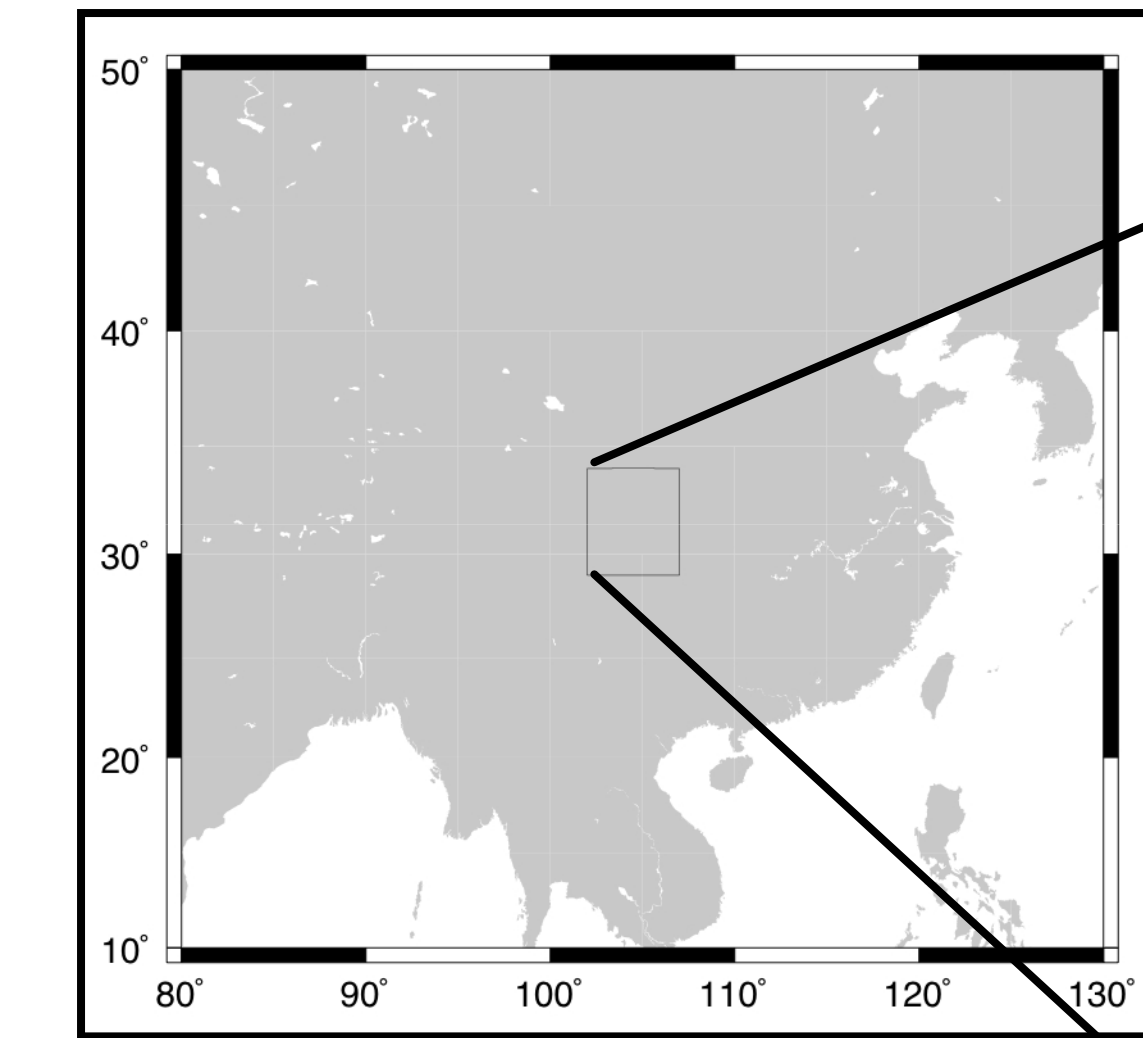
Technical Conclusions:

Large scale errors (> 20 km) are **dominated by ionospheric trends and waves** - these errors exceed 10 cm.

**Orbits should not be adjusted** since ALOS errors are < 5 cm and postseismic deformation will dominate.

Scansar-to-scansar is possible but unreliable because bursts must be aligned; **Swath-to-scansar provides the best space/time coverage for a great earthquake.**

Baselines should be **controlled to better than 200 m** to achieve adequate coherence in rugged areas.



## (2) Method

We use SIOSAR to process ALOS PALSAR data. The code has been revised to apply more precise orbit information. In addition we have developed scansar-to-scansar and scansar-to-strip capabilities. A layer-cake ionospheric correction has been developed using the global ionospheric (GIM) developed at JPL <http://iono.jpl.nasa.gov/gim.html>.

## (3) Strip interferometry

Ascending strip mode linterferograms (11.5 cm per fringe) from 72 scenes of ALOS PALSAR data. The red star is the main shock, the red circles are the magnitude 6 aftershocks on May 12th and May 25th, 2008 and the white circles are cities. The red line is the surface rupture mapped by Jing Liu of the Chinese Academy of Sciences.

While the lowland areas have good phase coherence, the phase recovery is decent in the mountain areas due to short baselines. Decorrelation is due to a combination of extreme shaking, temporal decorrelation from vegetation, and inadequate topographic phase correction in this area of extreme relief. Changes in the total electron content (TEC) of the ionosphere between the reference and repeat acquisitions causes a 1/2-fringe trend across most swaths.

## (4) Ionospheric effect on interferometry

The ionosphere has a significant effect on the propagation of radio-frequency electromagnetic radiation, especially at L-band. Consider a uniform change in the total electron content (TEC) of the ionosphere between the reference and repeat acquisition. Because the path through the ionosphere at the far end of the swath is greater than the path at the near end, the change in TEC will introduce a phase ramp of up to 1 fringe across each swath. This should **not** be confused with orbital baseline error. The change in phase across the swath is given by the following

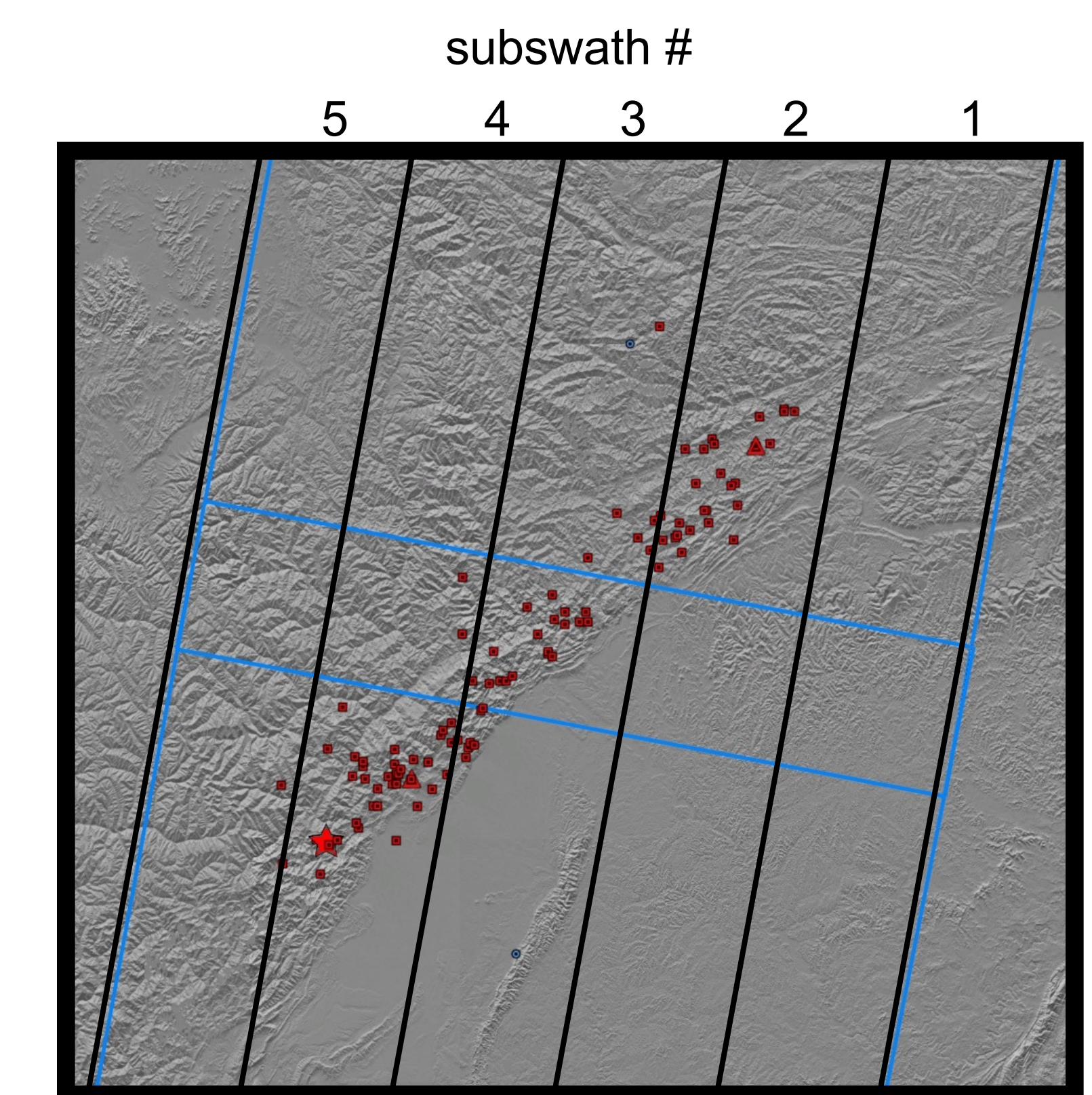
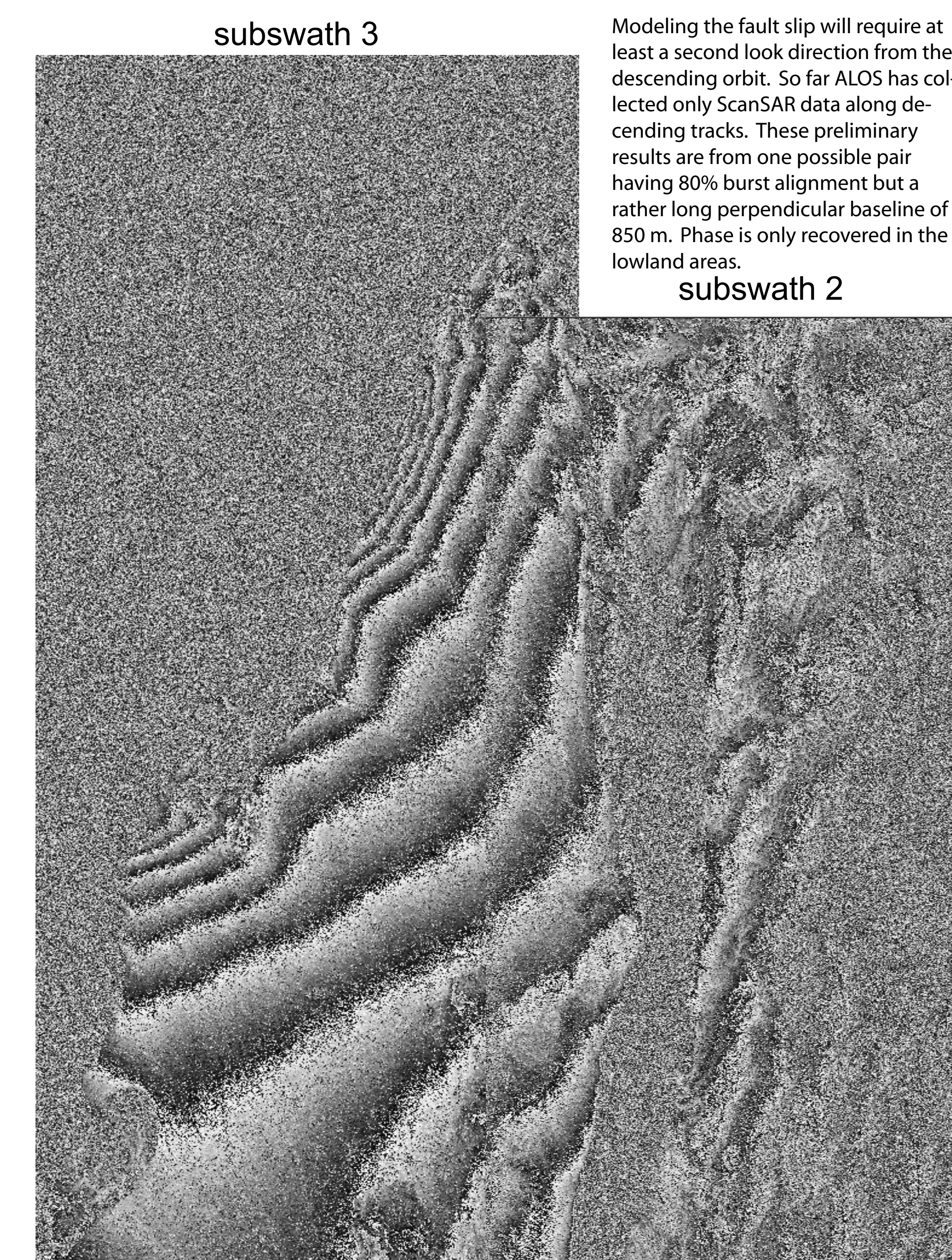
$$\Delta\phi = -N_T \left[ \frac{1}{\cos\theta_2} - \frac{1}{\cos\theta_1} \right] \frac{e^2\lambda}{2\pi\epsilon_0 m_e c^2} = -1.135 \text{ rad/TEC (L-band)}$$

$N_T$  - total electron content  
 $\theta_{2,1}$  - look angle at far and rear edge of swath (37°, 31°)  
 $e$  - electron charge  
 $m_e$  - electron mass  
 $\lambda$  - radar wavelength (0.236 m)  
 $c$  - speed of light

## (5) Acquisition date, perpendicular baseline, and ionospheric phase ramp for each track

Track	471	472	473	474	475	476
Dates of acquisition	Feb 29th 2008 ~ May 31 2008	Jan 28 2007 ~ Jun 17th 2008	Feb 17th 2008 ~ May 19th 2008	Mar 5th 2008 ~ Jun 5th 2008	Jun 20th 2007 ~ Jun 22nd 2008	Apr 8th 2008 ~ May 24th 2008
Approx. perpendicular baseline (m)	70	200	200	270	10	200
$\Delta\text{TEC}$ - ( $\times 10^{16}$ ele./m <sup>2</sup> )	2.1	3.0	5.2	0.7	-0.6	3.7
phase ramp in range (cm)	-3.9	-5.6	-9.8	-1.3	+1.1	-6.9

## (6) Preliminary scansar-to-scansar interferometry - (topographic phase not yet removed)



## (7) References

- Active tectonics of the Beichuan and Pengguan faults at the eastern margin of the Tibetan Plateau, Alexander, et al., Tectonics, VOL. 26, TC4500, doi:10.1029/2006TC001987, 2007
- A geological and geophysical context for the Wenchuan earthquake of 12 May 2008, Sichuan, People's Republic of China, Burchfiel, et al., GSA Today, VOL. 18, no. 7, doi:10.1130/GSATG18A.1, 2008
- Balmer, R. and M. Eineder, ScanSAR Processing Using Standard High Precision SAR Algorithms, IEEE Trans Geoscience and Remote Sensing, V. 34, P. 212-218, 1998.